Article

Radiation Balance over Low-Turbidity Water Artificially Cleaned for Irrigation of Tobacco Grown Under Shading. II. Water Albedo Analysis and Net Radiation Modelling

Tatyana Keyty de Souza Borges[1] (iD), Aureo Silva de Oliveira[2] (iD), Richard G. Allen[3] (iD),
Ayse Kilic[4] (iD), João Paulo Chaves Couto[2] (iD), Carlos Eduardo Santana[5]

[1]*Instituto Federal de Educação, Ciência e Tecnologia do Sertão Pernambucano, Ouricuri, PE, Brazil.*
[2]*Centro de Ciências Agrárias, Ambientais e Biológicas, Universidade Federal do Recôncavo da Bahia, Cruz das Almas, BA, Brazil.*
[3]*University of Idaho, Idaho, USA.*
[4]*University of Nebraska, Nebraska, USA.*
[5]*DANCO Comércio e Indústria de Fumos Ltda, Governador Mangabeira, BA, Brazil.*

Abstract

The albedo of a water surface and the energy available for evaporation are strongly correlated and studying such processes is of paramount importance for water security at farm and regional levels. In this paper, water albedo (α_w) and net all-wave radiation (R_n) were analyzed after being measured above the surface of an artificially cleaned and low-turbidity water used for tobacco irrigation. It was observed that α_w decreased as the sun elevation (θ) increased, especially for clear and near clear skies. The results showed that α_w can be reasonably predicted with a power law model either in terms of θ or S_g (incoming solar radiation) across different cloud cover conditions. From this study, a mean daily albedo of 0.05 is recommended. Three approaches were considered for estimation of daily R_n. In the first, a linear regression model strongly fitted R_n data in terms of S_g solely. The second option based on the definition of R_n was [$0.95S_g$ - $L_{net(56)}$], where $L_{net(56)}$ is net longwave (LW) radiation as used in the FAO56 model for reference evapotranspiration estimation, and the third was [$0.95S_g$ - $L_{net(MLR)}$], where MLR stands for multiple linear regression. The disadvantages of approaches (1) and (3), based on regressions, is that they are constrained to the type of water stored in the farm and the climatic conditions of the region. The performance of approach (2), where $L_{net(56)}$ is a widely used model, was comparable to the others can potentially be improved with a site-specific calibration. All three approaches for estimating daily R_n proposed in this study can possibily be extended to clear water that did not go through any filtration process.

Keywords: albedo, net radiation, water turbidity, tobacco.

Balanço de Radiação sobre Água de Baixa Turbidez Purificada Artificialmente para Irrigação de Fumo Cultivado sob Sombreamento. II. Análise do Albedo da Água e Modelagem da Radiação Líquida

Resumo

O albedo de uma superfície de água e a energia disponível para evaporação estão fortemente correlacionados e estudar tais processos é de suma importância para a segurança hídrica nível local e regional. Neste artigo, o albedo da água (α_w) e a radiação líquida (R_n) foram analisados após serem medidos acima da superfície de água artificialmente limpa e de baixa turbidez usada para irrigação de cultivo de fumo. Observou-se que α_w diminuiu com o aumento da elevação do sol

Corresponding author: Tatyana Keyty de Souza Borges. E-mail: tatyana.borges@ifsertao-pe.edu.br.

(θ), especialmente para céu limpo e quase limpo. Os resultados mostraram que α_w pode ser razoavelmente previsto com um modelo potencial em termos de θ ou S_g (radiação solar incidente) em diferentes condições de cobertura de nuvens. A partir deste estudo, um albedo médio diário de 0,05 é recomendado. Três abordagens foram consideradas para estimativa diária de R_n. Na primeira, um modelo de regressão linear ajustou-se fortemente aos dados de R_n em função de S_g, apenas. A segunda opção com base na definição de R_n foi [$0,95S_g$ - $L_{net(56)}$], onde $L_{net(56)}$ é a radiação líquida de onda longa do modelo FAO56 para estimativa da evapotranspiração de referência, e a terceira abordagem foi [$0,95S_g$ - $L_{net(MLR)}$], onde MLR significa regressão linear múltipla. As desvantagens das abordagens (1) e (3), baseadas em regressões, é que elas são restritas ao tipo de água armazenada na fazenda e às condições climáticas da região. O desempenho da abordagem (2), onde $L_{net(56)}$ é um modelo amplamente utilizado, foi comparável às outras e pode ser potencialmente melhorada com calibração local. Todas as três abordagens para estimar o R_n diário propostas neste estudo podem ser estendidas para águas claras que não passaram por nenhum processo de filtragem.

Palavras-chave: albedo, radiação líquida, turbidez da água, fumo.

1. Introduction

The radiation balance at a surface depends essentially on the time of day, the atmospheric conditions, and the nature of the surface (soil, water, vegetation, etc.). Time of day and cloud cover impact the magnitude of incoming radiation fluxes while the type of surface, described by its albedo (α) and emissivity (ε), affect the magnitude of outgoing fluxes while determining the amount of energy that can be absorbed by the surface and stored in the underlying medium.

The albedo of a water surface (α_w) varies over the course of a day and during the year because it is a function of solar elevation and thus the angle of the direct solar beam to the water surface (Finch and Hall, 2005). Adding to this, other factors strongly influence α_w such as the degree of cloudiness that affects the proportion of direct and diffuse radiation, water quality, and state of the surface, like height and orientation of waves, which in turn are related to the speed and direction of wind over water (Henderson-Sellers and Hughes, 1982; Katsaros *et al.*, 1985; Jin *et al.*, 2004; Liu *et al.*, 2015). Studies on α_w have typically been restricted to oceans (Payne, 1972; Cogley, 1979; Katsaros *et al.*, 1985; Feng *et al.*, 2016). Over a freshwater lake in Canada, Nunez *et al.* (1972) reported α_w varying from 0.07 to 0.11 on a daily basis. Typical values for α_w encompassing variable cloud cover conditions (from clear to overcast skies) are in the range of 0.10-0.50 at low sun and 0.03 to 0.10 at high sun (Shuttleworth, 2012). A mean value of α_w for deep water is in the range of 0.04-0.08 (Jensen and Allen, 2016). Henderson-Sellers (1986) discussed several approaches for estimating α_w. Vitale *et al.* (2019) successfully fitted seasonal data to sinusoidal functions to estimate α_w in terms of month of the year over an intertidal wetland.

Detailed information on the radiation balance at a water surface can be obtained by a four-component net radiometer mounted above the surface. With such instrument, the albedo and the net all-wave radiation (R_n) can be derived from measurements of the shortwave and longwave components. But net radiometers are expensive and delicate instruments that require careful handling to attain accurate measurements (Myeni *et al.*, 2020). Therefore, it is desirable to estimate R_n over water.

Henderson-Sellers (1986) reviewed several methods for calculating R_n within the context of open water evaporation modelling. Recently, Myeni *et al.* (2021) has investigated the performance of a model that uses land-based meteorological data to calculate R_n over open water surfaces. The importance of simple and reliable models for estimating R_n over water has been emphasized (Mengistu and Savage, 2017; Myeni *et al.*, 2021). Incoming and net shortwave radiation fluxes have been shown to be good estimators of R_n under both clear and cloudy conditions and for a wide range of surfaces, including water (Alados *et al.*, 2003). El-Bakry (1994) reported regression coefficients for estimation of R_n using incoming SW radiation at the Aswan High Dam Lake in Egypt and Li and Barnes (1980) developed similar relationships for Lake Albert in South Australia. Jensen *et al.* (1990) made a compilation of linear regression coefficients for estimating R_n for various cropped surfaces.

Storage of water in natural lakes, impoundments and farm reservoirs is of great importance to ensure water security. Around the world, huge amounts of water are lost every year from these water storages mainly in tropical regions and the study of the radiation balance at such surfaces help to develop programs for water conservation and management at local and regional levels. The purpose of this paper was to analyze the albedo of low-turbidity water stored in an agricultural reservoir for irrigation purposes. Measurements of all components of the radiation balance over two seasons provided enough data for modelling R_n over the water surface.

2. Material and Methods

A detailed description of the experimental site and the instrumentation used is presented in the first paper of this series, hereafter referred to as Part I. In summary, measurements of all components of the radiation balance were made over low-turbidity water used for irrigation of tobacco plants grown under shading in the east of Bahia. Experimental data were collected during the second parts

of 2015 and 2016 using instruments mounted on-board a handmade floating platform as described by Borges *et al.* (2016) and Borges (2017), positioned in the center of an artificial reservoir.

A four-component net radiometer (model CNR4, Kipp & Zonen) measured continuously the incident and the outgoing shortwave (SW) and longwave (LW) radiation fluxes. Data were collected with dataloggers (model CR1000, Campbell Scientific) and stored in intervals of 5 min, 30 min, 60 min, and 1440 min, for further analysis. From the SW components, the water albedo α_w was calculated according to Eq. (1), being albedo the ratio between reflected and incoming SW radiation.

$$\alpha_w = \frac{S_r}{S_g} \qquad (1)$$

where α_w is the water surface albedo (dimensionless), S_r is the reflected SW radiation by the surface and S_g is the incoming SW radiation.

In the datalogger, the measured net all-wave radiation R_n was calculated from the four components according to Eq. (2).

$$R_n = S_{net} + L_{net} = \left(S_g - S_r\right) + \left(L_{atm} - L_{out}\right) \qquad (2)$$

where S_{net} is the net SW radiation, L_{net} is the net LW radiation, L_{atm} is the incoming LW radiation from the atmosphere, and L_{out} is the outgoing LW radiation from the surface. All terms in Eq. (2) are given in W/m^2.

Here is used the same criteria and selected days mentioned in Part I regarding the effects of cloud cover on the radiation balance components through the mean day-time atmospheric transmissivity τ_{atm} for SW radiation.

2.1. Modelling of net radiation fluxes

In this Part II, approaches for modelling net SW radiation (S_{net}), net LW radiation (L_{net}), and R_n are tested and evaluated based on daily observation of incoming SW radiation from the net radiometer and air temperature and relative humidity measured at the weather tower deployed in a row between the irrigation reservoirs during both 2015 and 2016 campaigns. Models to estimate the components of the radiation balance from atmospheric variables tend to use data commonly obtained with standard weather stations and from historical daily weather data sets. In the tobacco farm, for example, such models can be used to evaluate water loss by evaporation from the open water surfaces, an important information for implementation of a water management program.

The net SW radiation flux was estimated from S_g according to Eq. (3).

$$S_{net(e)} = (1 - \alpha_{wc})S_g \qquad (3)$$

where $S_{net(e)}$ is the estimated daily net SW radiation (W/m^2) based on a constant value for water surface albedo (α_{wc}) and S_g is the daily incoming SW radiation from the net radiometer (W/m^2).

Two approaches were considered to estimate L_{net}: (i) the same used in the FAO Penman-Monteith equation (Allen *et al.*, 1998) to calculate reference evapotranspiration (Eq. (4)) and (ii) a multiple linear regression model having as input variables air temperature, relative humidity, and an indicator of daytime relative cloudiness.
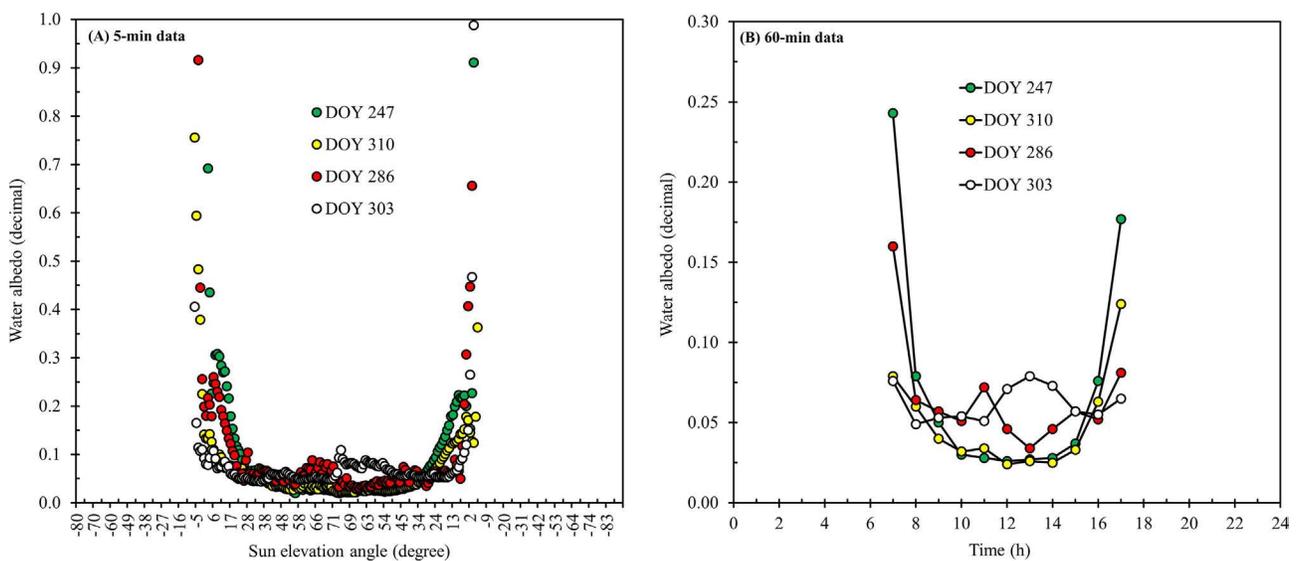
Figure 1 - Daily course of the low-turbidity water albedo α_w for the four selected days with contrasting cloud cover. DOY 247/2015 (CSS, τ_{atm} = 0.72), DOY 310/2016 (MSS, τ_{atm} = 0.55), DOY 286/2016 (MCS, τ_{atm} = 0.36), and DOY 303/2015 (CCS, τ_{atm} = 0.18). CSS = completely sunny (clear) sky, MSS = mostly sunny sky, MCS = mostly cloudy sky, and CCS = completely cloudy (overcast) sky.

$$L_{net(56)} = \sigma\left(\frac{T_x^4 + T_n^4}{2}\right)(0.14 - 0.34\sqrt{e_a}) \times$$

$$\left(1.35\frac{S_g}{S_{go}} - 0.35\right) \qquad (4)$$

where $L_{net(56)}$ is the estimated daily net LW radiation (W/m^2) according to FAO 56 paper (Allen *et al.*, 1998), σ is the Stefan-Boltzmann constant (5.67x10^{-8} W/m^2.K^4), T_x is the daily maximum air temperature (K), T_n is the daily minimum air temperature (K), e_a is the daily mean actual vapor pressure (kPa), S_g and S_{go} are as previously defined. The ratio S_g/S_{go} represents relative cloudiness and in Eq. (4) is limited to $0.25 < S_g/S_{go} \le 1.0$ (ASCE, 2005).

The multiple linear regression technique (MLR) allows the investigation of an association among three or more variables (Akritas, 2016) and is generally written as an equation relating the response variable Y to the predictor variables $X_1,\ldots, X_k$ and an intrinsic error variable (ε) as given in Eq. (5).

$$Y = \beta_0 + \beta_1 X_1 + \ldots + \beta_k X_k + \varepsilon \qquad (5)$$

where β_0 is the intercept and β_i ($i = 1, 2,\ldots, k$) are the multiple regression coefficients of the dependent variable Y on the independent variable X_i ($i = 1, 2,\ldots, k$).

In the present study, atmospheric parameters readily available from standard weather stations and commonly associated to the exchange of LW radiation between the surface and the atmosphere were considered as candidates for independent variables in the MLR model. The model was parameterized with data from 2015 using a stepwise procedure in R (R Core Team, 2017) and validated with the data collected in 2016. The objective of such a procedure is arriving at an optimal prediction equation by using statistical criteria to eliminate unnecessary predictors leading to the final form of the regression model that includes only those predictor variables that can explain the observed variability in the dependent variable.

Finally, three approaches were considered for modelling net all-wave radiation R_n. The first, consisted in using incoming SW radiation S_g to predict R_n by means of a simple linear regression. This method has been widely used over different types of surfaces including water (Sene *et al.*, 1991; El-Bakry, 1994). As the first approach, in this paper R_n was modelled using $S_{net(e)}$ as the predictor variable, according to Eq. (6). The second (Eq. (7)) and third (Eq. (8)) approaches followed the definition of R_n as the sum of net SW and net LW radiation fluxes. Initially, R_n was given as the sum of Eqs. (3) and (4) and then as the sum of Eqs. (3) and (5).

$$R_{n(1)} = a_0 + a_1 S_{net(e)} \qquad (6)$$

$$R_{n(2)} = S_{net(e)} - L_{net(56)} \qquad (7)$$

$$R_{n(3)} = S_{net(e)} - L_{net(MLR)} \qquad (8)$$

where $R_{n(1,2,3)}$ is the estimated daily net all-wave radiation (W/m^2), a_0 and a_1 are regression coefficients, and $L_{net(MLR)}$ is the estimated daily net LW radiation with the multiple linear regression model.

3. Results and Discussion

3.1. Albedo of the water surface

In this paper, daily water surface albedo (α_w) was calculated as the ratio of 24-h mean values of S_r to S_g in W/m^2. In 2015, the daily α_w varied from 0.034 to 0.072 with an average of 0.050 and in 2016 it varied from 0.031 to 0.067 with an average value of 0.044. Considering both years, the daily mean α_w was 0.047. Albedo generally increased to above 0.06 on cloudy days and decreased to near 0.03 on relatively clear days. These results are consistent with Finch and Hall (2005) and Jensen and Allen (2016) who highlighted the low average value of water albedo (0.06) compared to other surfaces, like vegetation. In agricultural crops, for example, mean albedo in the range of 0.20 to 0.25 area recommended. Henderson-Sellers (1986) and Shutlleworth (2012) suggest a mean albedo of 0.08 for water including effects of cloud cover.

Figure 1 shows the daily course of α_w for the four days selected in Part I with contrasting atmospheric transmissivity (τ_{atm}) as follows: $\tau_{atm} = 0.72$ (DOY 247/2015), $\tau_{atm} = 0.55$ (DOY 310/2016), $\tau_{atm} = 0.36$ (DOY 286/2016), and $\tau_{atm} = 0.18$ (DOY 303/2015). In Fig. 1A, α_w is given as a function of sun elevation angle (θ) in the range of 0 to 90° using 5-min data, while in Fig. 1B, hourly values were plotted as a function of local time. Clearly, α_w tended to decrease as θ increased, a pattern extensively reported in other studies (Katsaros *et al.*, 1985; Jin *et al.*, 2004; Liu *et al.*, 2015). Most of the albedo data plotted in Fig. 1A are below 0.30. However, high α_w values (> 0.50) occurred with low θ at sunrise and sunset regardless of cloud cover conditions. It is difficult to interpret albedo values occurring early in the morning and late afternoon. It is known that, physically, sun glint is a phenomenon that causes the very high values of α_w at these times under clear sky conditions. It is also possible that albedo was impacted, to some degree, by sensor oscillation in the raft in windy days and sides of the water reservoir at low θ.

In Fig. 1B, U-shape curves are seen on clear and near clear days (DOY 247 and 310), with maximums occurring early in the morning and late afternoon when

sun angles were low, and minimums occurring around noon when sun angles were the highest. Under high atmospheric transmissivity, a well-defined relationship between water albedo and time was observed (Nunez *et al.*, 1972; Henderson-Sellers, 1986; Liu *et al.*, 2015). On the other hand, Fig. 1B also shows that as the degree of cloudiness increased, the U-shape pattern changed so that the timing of maximum and minimum α_w values became more difficult to predict and α_w amplitude decreased.

The four days in Fig. 1 comprise a representative range of conditions for τ_{atm} (from 0.18 to 0.72) in the region, so it was expected that the average α_w for these particular days was similar to the mean value (0,047) for both seasons. The daily albedo computed using mean daily values of S_g and S_r (see Table 3 in Part I) were 0.045 for DOY 247, 0.038 (DOY 310), 0.054 (DOY 286), and 0.061 (DOY 303), with an overall average of 0.049.

Table 1 shows adjustments of a power-law model for estimation of α_w in terms of θ and incoming SW radiation (S_g), which by itself is a function of θ. Five-min average data were used to calibrate the model. Generally, the coefficient of determination (r^2) decreased as cloud cover increased. For the case of all-cloud cover condition in Table 1, the model predicts α_w varying from 0.25 to 0.03 in the θ interval from 5° to 90°, whose values are within the range of measured albedo over the low-turbidity water during both the 2015 and 2016 seasons.

In order to investigate the influence of τ_{atm} on α_w, the two extreme cases of cloud cover (CCS and CSS) were considered based on the 5-min data sets of both years. Before processing the raw data, a quality control procedure was applied as follows: (i) all data were deleted from the series when the calculated τ_{atm} was not a number, $\tau_{atm} \leq 0$ or $\tau_{atm} \geq 1$; (ii) all data were deleted when calculated θ was not a number or $\theta \leq 0$; (iii) all data were deleted when α_w was not a number or when $\alpha_w \leq 0$ or $\alpha_w > 1$; and (iv) all data were deleted when $R_n < 0$.

As previously discussed in Fig. 1 and according to Katsaros *et al.* (1985) and Jin *et al.* (2004), Fig. 2A illustrates that under high sun elevation above the horizon and with flat water surface, the albedo for water tends to be higher in the presence of clouds (overcast and near overcast skies), as the diffuse, multi-direction SW radiation in the atmosphere increases the mean angle of incidence of radiation from the vertical and the effect of solar elevation is considerably dampened. In the absence of clouds (clear sky and near clear skies) the incidence angle from vertical is small and the albedo is lowest under high sun elevation. The opposite occurs when the sun is low above the horizon ($\theta < 30°$). In this condition, the albedo tends to be larger in the absence of clouds and decreases sharply with sun angle, as the angle of incidence of the radiation beam from vertical becomes smaller.

Figure 2A also shows that, for a given sun elevation angle, the variability in α_w under dense cloud cover was substantially higher. This higher variability can be a combined effect of the state of the surface (lack of flatness due to wind blowing) and diffuse radiation reaching the surface in larger proportions compared to the direct beam. It is interesting to observe that from around 25° to 35° of sun elevation, the two extreme cloud cover data sets tended to intersect and the relationship between α_w and θ seems to be less dependent on the degree of cloudiness. A second plot (Fig. 2B) was developed to explore how water albedo relates to the full range of τ_{atm} for a set of arbitrarily chosen θ intervals. In Fig. 2B, the albedo of the low turbidity water was very sensitive to changes in τ_{atm} under low sun elevation angle ($\theta \leq 10°$). In this range, α_w increased rapidly as τ_{atm} increased, most likely due to larger sunglint from the greater amount of direct sun beam at higher τ_{atm}. In the θ range from 25° to 35°, α_w was essentially constant across the τ_{atm} values, pattern also reported by Oke (1995). At higher θ values (> 50°), the water albedo shows a slightly decreasing pattern with atmospheric transmissivity, with lowest values of α_w toward clear sky in accordance with Fig. 2A.

3.2. Models for estimating net radiation fluxes

Modelling net radiation fluxes from commonly measured weather data makes the determination of radiation balance more viable and independent of high-cost and delicate instrumentation. It also increases the ability to apply the methodology using historical data sets. The proposed approach to predict net SW radiation for the low-turbidity water (Eq. (3)) is simplified and made more general by requiring only a knowledge of α_{wc}, as a constant value for water albedo. On a daily basis, the α_{wc} adopted here is 0.05, which is the average water surface albedo for both years calculated from 24-h S_r and S_g fluxes. This value was also obtained from measured S_{net} data (totaling 189 points of daily data from both years) that were plotted against $S_{net(e)}$ and α_w was successively changed until the best fitting (Y = 1.0007·X, coefficient of determination r^2 = 0.99996, and standard error of estimate SEE = 1.53 W/m²) was obtained, which occurred when α_{wc} was set equal to 0.047 or about 0.05.

Tabla 1 - Coefficients for the power-law fitting for estimating the low-turbidity water surface albedo (α_w) in a tropical climate from incident SW radiation flux (S_g) in W/m² and sun elevation angle (θ) in degree.

Cloud cover conditions	$\alpha_w = A(\theta)^B$			$\alpha_w = C(S_g)^D$		
	A	B	r^2	C	D	r^2
All	0.8563	-0.771	0.70	1.1324	-0.521	0.53
CSS	1.3842	-0.931	0.68	75.552	-1.147	0.67
MSS	1.5587	-0.921	0.86	28.594	-1.019	0.83
MCS	0.2938	-0.469	0.56	0.6849	-0.461	0.48
CCS	0.1524	-0.239	0.20	0.3104	-0.335	0.36

CSS = completely sunny (clear) sky, MSS = mostly sunny sky, MCS = mostly cloudy sky, and CCS = completely cloudy (overcast) sky.
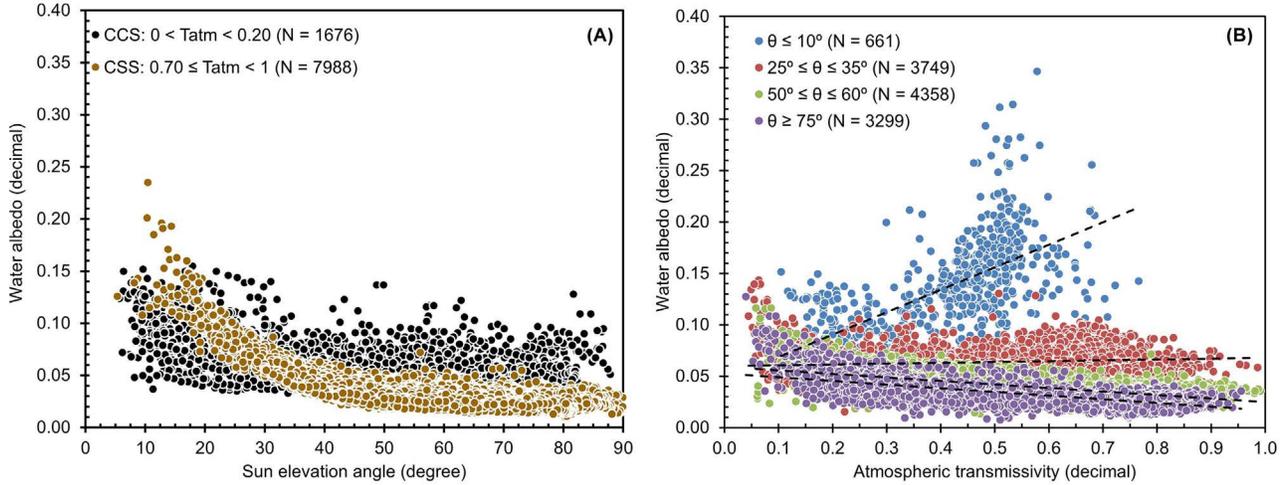
Figure 2 - Plot of low-turbidity water albedo against sun elevation angle for the two extreme conditions of cloud cover (A) and against atmospheric transmissivity for SW radiation for four intervals of sun elevation angle (B).

Once α_w was defined, the net SW radiation flux was then modelled from S_g measured at the weather station as $S_{net(e)} = 0.95 \cdot S_g$, which means that on average, 95% of the daily SW radiation incident over the clear water surface in the irrigation reservoirs tended to be absorbed. Therefore, compared to other natural surfaces, clear water is on average one of the most effective absorbing mediums of SW solar radiation (Katsaros *et al.*, 1985; Oke, 1995; Jensen and Allen, 2016).

As mentioned previously, two approaches were applied to model net LW radiation, the FAO56 equation without site-specific calibration (Eq. (4)) and a multiple linear regression model (Eq. (5)) using atmospheric data from a standard automatic weather station as the predictor variables. The inputs to the FAO56 L_{net} model (Allen *et al.*, 1998) are T_x (maximum air temperature, K), T_n (minimum air temperature, K), e_a (actual vapor pressure, kPa), and the S_g/S_{go} ratio (relative cloudiness index, dimensionless). Based on daily data from 2015 (135 data points), it was found that $L_{net(56)}$ underestimated measured values for water by about 30%, with a mean ratio between estimated and measured L_{net} equal to 0.70 (max = 1.32, min = 0.18, standard deviation, sd = 0.18). Measured L_{net} was plotted against $L_{net(56)}$ resulting in a linear regression fitting (Y = A + B·X) with the following parameters: A = 24.91 W/m², B = 0.7734, r² = 0.608, and SEE = 7.99 W/m². One data point (30th October) was excluded from this analysis because the condition of $S_g/S_{go} > 0.25$ was violated.

The same 2015 set of daily data was used to derive the coefficients for the multiple linear regression (MLR) model. Several weather variables commonly associated to the exchange of LW radiation between surface and atmosphere were considered, such as T_x (°C), T_n (°C), e_a (kPa), S_g/S_{go} (dimensionless), mean air temperature (T_m, °C)

given as $(T_x + T_n)/2$, maximum relative humidity (RH$_x$, %), minimum relative humidity (RH$_n$, %), air temperature amplitude (ΔT, °C), and vapor pressure deficit (*VPD*, kPa). Fourth-degree powers of T_x and T_n were also considered, as in the FAO56 L_{net} model following the Stefan-Boltzmann law. These variables were tested as a single input and in pairs in the form of products. After many runs, the best fitting relationshiop (r² = 0.721, SEE = 6.87 W/m²) was obtained when measured daily L_{net} was expressed as a function of T_x (°C), T_n (°C), RH_x (%), RH_n (%), and S_g/S_{go} according to Eq. (9).

$$L_{net(MLR)} = 8.661 + 1.077(T_x) - 3.334(T_n) +$$

$$0.947(RH_x) - 0.480(RH_n) + 26.869\left(\frac{S_g}{S_{go}}\right) \qquad (9)$$

Different from the FAO56 L_{net} model, in Eq. (9) the S_g/S_{go} ratio is allowed to be lower than or equal to 0.30 since values in this range were used for derivation. Validation of $L_{net(MLR)}$ against daily data obtained in 2016 (independent data set with N = 54) showed a linear regression fitting through the origin (Y = B·X) with a high coefficient of determination (r² = 0.986), slope near 1 (B = 0.981), and a small standard error of estimate (SEE = 6.76 W/m²).

Figure 3 depicts the course of measured and estimated net LW radiation for the year 2016 by both methods. This plot is a form of validation for the FAO56 L_{net} approach that could not be done in the same way that was done for the multiple linear regression, since the original constants in that approach were not changed. It is interesting to observe that both sets of estimated data not only agree with each other, but also agree with the measured values for L_{net}. Basically, both FAO56 and MLR approaches concomitantly produced an overestimation or underestimation of measured L_{net} values. Like in 2015, the ratio
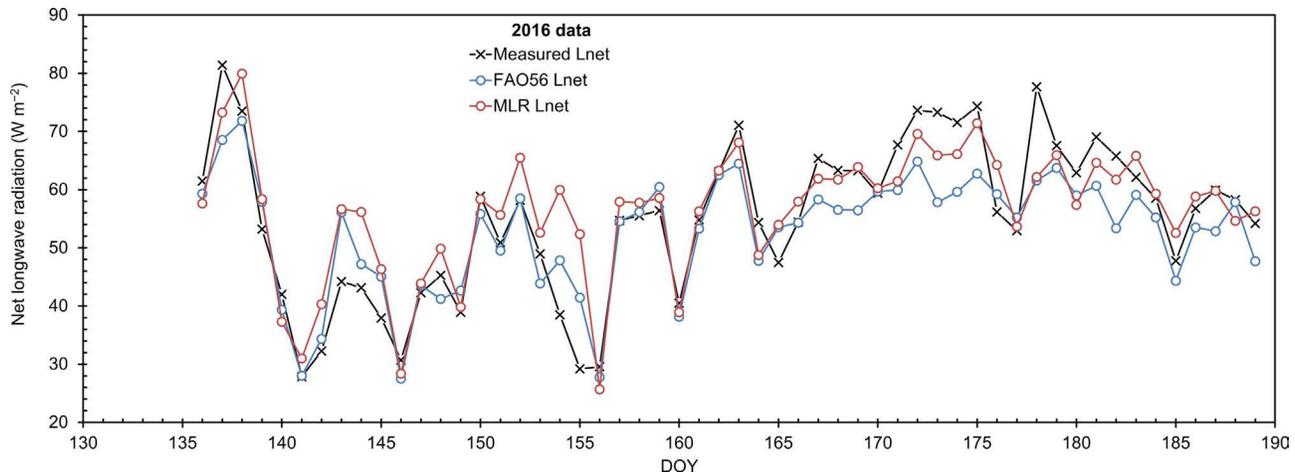
Figure 3 - Course of measured and estimated daily net longwave radiation over the low-turbidity water surface in 2016 from DOY 136 to DOY 189 (54-day interval).

between estimated and measured L_{net} in 2016 was lower than 1 (0.61 on average, max = 0.91, min = 0.11, sd = 0.16) for the FAO56 L_{net} model and 1.04 (max = 1.79, min = 0.80, sd = 0.16) for the MLR model. Therefore, the use of Eq. (9) to estimate the net outgoing LW radiation from the low turbidity water seems to be a better option as compared to the FAO56 L_{net} model. The better performance for the $L_{net(MLR)}$ was expected, since the regression is tailored to the experimental data. Because of this, the $L_{net(MLR)}$ is not universal, which means that it cannot be applied to similar water surfaces under climatic conditions that might differ substantially from those encountered in the east of Bahia region.

The FAO56 equation (Eq. (4)) for estimating L_{net} was developed for vegetated surfaces in the context of crop water requirement studies (Wright, 1982; Burman and Pochop, 1994; Allen *et al.*, 1998). That equation assumes an emissivity of 0.98 for the soil-vegetation mixture and the calculation of net emissivity with the Brunt (1932) model. The mixture emissivity is similar to that recommended for water surfaces (ε_w = 0.97) (Davies *et al.*, 1971; Konda *et al.*, 1994; Jensen and Allen 2016). On the other hand, the FAO56 equation uses air temperature at screen height to estimate both incoming and outgoing LW radiation and the equation is recommended for computation of reference crop evapotranspiration (Jensen *et al.*, 1990; Jensen and Allen, 2016). But Fig. 4B in Part I shows that, under the same environmental conditions, differences between water temperature T_w and air temperature T_a can be significant over the course of a day. Such differences might explain the inability of the FAO56 L_{net} equation to predict L_{net} over the low turbidity water surface in the experimental area of this study. In order to improve the estimates with this equation, one option would be a site-specific calibration by adjusting the coefficients for net emissivity and the cloud cover factor to account for local conditions (Kjaersgaard *et al.*, 2007; Wu *et al.*, 2017; Kofronova *et al.*, 2019).

Net all-wave radiation R_n was modelled following three approaches (Eqs. (6) to (8)). In the first one, $S_{net(e)}$ = 0.95·S_g was taken as the predictor variable and Eq. (10) is the result of the linear regression analysis that produced a model with a high correlation (r^2 = 0.951 and SEE = 9.66 W/m^2), since R_n is closely correlated with net SW radiation, which in turn is closely correlated with S_g. Derivation of Eq. (10) used data from 2015 (N = 135) and was restricted to $S_{net(e)}$ values from about 79 W/m^2 to 306 W/m^2. Validation with the 2016 data set (N = 54) showed a linear model passing through the origin (Y = B·X) with B = 1.034, r^2 = 0.998, and SEE = 7.56 W/m^2.

$$R_{n(1)} = -21.357 + 0.832 \cdot S_{net(e)} \qquad (10)$$

Figure 4 compares measured daily R_n with calculated values obtained with the approaches $R_{n(2)}$ (Eq. (7)) and $R_{n(3)}$ (Eq. (8)). A better agreement between measured and estimated R_n was obtained with the $R_{n(3)}$ approach (Fig. 4B), where the y-intercept is closer to 0, the slope is closer to 1 and SEE is 7.37 W/m^2, about 33% lower than the SEE in Fig. 4A. The ratio of estimated $R_{n(2)}$ to measured R_n [$R_{n(2)}/R_n$] averaged 1.13 while for the ratio $R_{n(3)}/R_n$ the average was 1.01, suggesting that R_n calculated with the FAO56 L_{net} model overestimated measured R_n in 13%, on average.

The use of a well-fitted simple linear regression to estimate R_n over water surface in terms of incoming SW radiation or net SW radiation is a valid option where data on solar radiation are available and the water clearness remains fairly constant over time, which is the case for the experimental area of this study. In the tobacco farm, every year from April to August, the tanks are refilled with clean
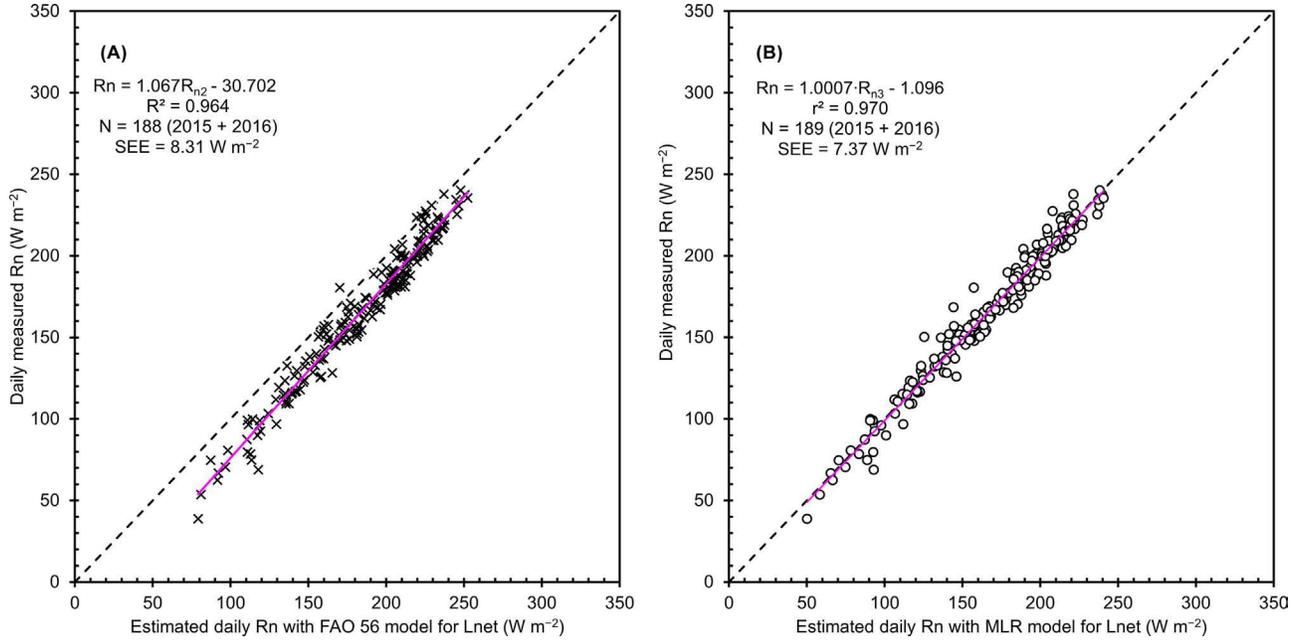
Figure 4 - Measured all-wave net radiation against calculated net-all wave radiation with $L_{net(56)}$ (A) and with $L_{net(MLR)}$ (B), where 56 stands for FAO 56 Penman-Monteith equation and MLR stands for multiple linear regression model.

water coming from the filtration system to supply crop demand during the next irrigation season (September to March). If a nearby land-based weather station also provides data on other parameters such as air temperature (maximum and minimum) and relative humidity (maximum and minimum) that can be used with the Eq. (9), then the $R_{n(3)}$ approach becomes a viable option for estimation of R_n over the water surface in the irrigation tanks, as part of a program to maximize the water management in the farm. On the other hand, improvements in $R_{n(2)}$ can be achieved with the application of a site-specific calibration for the FAO56 L_{net} model.

4. Final Considerations

This is the Part II of the paper series on the radiation balance measured with a four-component net radiometer above an open low-turbidity water used for irrigation of tobacco plants in the east of Bahia, Brazil. The focus here was to analyze the surface albedo and model the net shortwave (SW) radiation (S_{net}), the net longwave (LW) radiation (L_{net}), and the net all-wave radiation (R_n) on a daily basis.

It was observed that water albedo (α_w) tended to decrease as the sun elevation (θ) increased, especially for clear skies and near clear skies. Under such conditions, a well defined U-shape curve was found with minimum hourly α_w occurring around noon. This pattern was not so evident under cloudy and near cloudy skies. The results showed that α_w can be reasonably predicted with a power law model either in terms of θ or S_g (incoming SW radia-

tion) across different cloud cover conditions. Under cloudy sky, α_w was higher for θ above 25°-30° compared to clear sky. Below that, α_w was higher for clear sky conditions. For the low-turbidity water, a mean daily albedo of 0.05 is recommended from this study, so net SW radiation was modelled as $0.95S_g$. Net LW radiation was successfuly modelled with the multiple linear regression (MLR) technique, where $L_{net(MLR)}$ was expressed as a function of five input variables commonly measured in standard weather stations. Similar performance was not obtained with $L_{net(56)}$, which is the FAO56 model for net LW radiation used in crop evapotranspiration.

Three approaches were considered for estimation of daily R_n. In the first approach, a linear regression model strongly fitted R_n data in terms of S_g solely. The second option based on the definition of R_n was [$0.95S_g - L_{net(56)}$] and the third was [$0.95S_g - L_{net(MLR)}$]. The disadvantages of approaches (1) and (3), based on regressions, is that they are constrained to the type of water used for irrigating the tobacco crop and the climatic conditions of the region, as well. The performance of approach (2), an universal model, was comparable to the others and can potentially be improved with a site-specific calibration. All three approaches for estimating daily R_n proposed in this study can possibily be extended to clear water that did not go through any filtration process.

Acknowledgments

References

AKRITAS, M. **Probability and Statistics with R for Engineers and Scientists**. New York: Pearson, 513 p., 2016.

ALADOS, I.; FOYO-MORENO, I.; OLMO, F.J.; ALADOS-ARBOLEDAS, L. Relationship between net radiation and solar radiation for semi-arid shrub-land. **Agricultural and Forest Meteorology**, v. 116, n. 3-4, p. 221-227, 2003. doi

ALLEN, R.G.; PEREIRA, L.S.; RAES, D.; SMITH, M. **Crop Evapotranspiration: Guidelines for Computing Crop Water Requirements. Irrigation and Drainage Paper 56**. Rome: FAO, 1998.

ASCE. **The ASCE Standardized Reference Evapotranspiration Equation**. Reston: ASCE, 205 p., 2005.

BORGES, T.K.S. **Evaporação em Superfície de Água Livre com Baixa Turbidez**. Tese de Doutorado em Engenharia Agrícol, Universidade Federal do Recôncavo da Bahia, Cruz das Almas, 120 p., 2017.

BORGES, T.K.S.; OLIVEIRA, A.S.; SILVA, N.D.; SANTANA, C.E. Plataforma flutuante de baixo custo para pesquisas em micrometeorologia e qualidade da água em reservatórios. **Revista Geama**, v. 4, n. 1, p. 38-45, 2016.

BURMAN, R.; POCHOP, L.O. **Evaporation, Evapotranspiration and Climatic Data**. Amsterdam: Elsevier, 278 p., 1994.

BRUNT, D. Notes on radiation in the atmosphere. **Quarterly Journal of Royal of Meteorological Society**, v. 58, n. 247, p. 389-420, 1932. doi

COGLEY, J.G. The albedo of water as a function of latitude. **Monthly Weather Review**, v. 107, n. 6, p. 775-781, 1979. doi

DAVIES, J.A.; ROBISON, P.J.; NUNEZ, M. Field determinations of surface emissivity and temperature for Lake Ontario. **Journal of Applied Meteorology**, v. 10, n. 4, p. 811-819, 1971. doi

EL-BAKRY, M.M. Net radiation over the Aswan High Dam Lake. **Theoretical and Applied Climatology**, v. 49, n. 3, p. 129-133, 1994. doi

FENG, Y.; LIU, Q.; QU, Y.; LIANG, S. Estimation of the ocean water albedo from remote sensing and meteorological reanalysis data. **IEEE Transactions on Geosciences and Remote Sensing**, v. 54, n. 2, p. 850-868, 2016. doi

FINCH, J.W.; HALL, R.L. Evaporation from lakes. In: ANDERSON, M. G.; McDONNEL, J. J. (Org.). **Encyclopedia of Hydrological Sciences**. Chichester: Wiley, p. 635-646, 2005.

HENDERSON-SELLERS, B. Calculating the surface energy balance for lake and reservoir modeling: A review. **Reviews of Geophysics**, v. 24, n. 3, p. 625-649, 1986. doi

HENDERSON-SELLERS, A.; HUGHES, N.A. Albedo and its importance in climate theory. **Progress in Physical Geography: Earth and Environment**, v. 6, n. 1, p. 1-44, 1982. doi

JENSEN, M.E.; ALLEN, R.G. **Evapotranspiration and Irrigation Water Requirements. Manuals and Reports on Engineering Practice 70**. New York: ASCE, 360 p., 1990.

JENSEN, M.E.; ALLEN, R.G. **Evaporation, Evapotranspiration and Irrigation Water Requirements. Manuals and Report on Engineering Practice 70**. Reston: ASCE, 769 p., 2016.

JIN, Z.; CHARLOCK, T.P.; SMITH JR, W.L.; RUTLEDGE, K. A parameterization of ocean surface albedo. **Geophysical Research Letters**, v. 31, n. 22, p. 1-4, 2004. doi

KATSAROS, K.B.; McMURDIE, L.A.; LIND, R.L.; DEVAULT, J.E. Albedo of a water surface, spectral variation, effects of atmospheric transmittance, sun angle and wind speed. **Journal of Geophysical Research**, v. 90, n. C4, p. 7313-7321, 1985. doi

KONDA, M.; IMASATO, N.; NISHI, K.; TODA, T. Measurement of the sea surface emissivity. **Journal of Oceanography**, v. 50, p. 17-30, 1994. doi

KJAERSGAARD, J.H.; CUENCA, R.H.; PLAUBORG F.L.; HANSEN, S. Long-term comparisons of net radiation calculation schemes. **Boundary-Layer Meteorology**, v. 123, n. 3, p. 417-431, 2007. doi

KOFRONOVA, J.; MIROSLAV, T.; SIPEK, V. The influence of observed and modelled net longwave radiation on the rate of estimated potential evapotranspiration. **Journal of Hydrology and Hydromechanics**, v. 67, n. 3, p. 280-288, 2019. doi

LI, C.W.; BARNES, I.W. The relationship between net and global radiation over water. **Theoretical and Applied Climatology**, v. 28, n. 1-2, p. 91-100, 1980. doi

LIU, H.; FENG, J.; SUN, J.; WANG, L.; XU, A. An eddy covariance measurements of water vapor and CO_2 fluxes above the Erhai Lake. **Science China Earth Sciences**, v. 58, n.3, p. 317-328, 2015. doi

MYENI, L.; MOELETSI, M.E.; CLULOW, A.D. Assessment of three models for estimating daily net radiation in southern Africa. **Agricultural Water Management**, v. 229, 105951, 2020. doi

MYENI, L.; SAVAGE, M.J.; CLULOW, A.D. Modelling daily net radiation of open water surfaces using land-based meteorological data. **Water SA**, v. 47, n. 4, p. 498-504, 2021. doi

NUNEZ, M.; DAVIES, J.A.; ROBINSON, P.J. Surface albedo at a tower site in Lake Ontario. **Boundary-Layer Meteorology**, v. 3, n. 1, p. 77-86, 1972. doi

OKE, T.R. **Boundary Layer Climates**. London: Routledge, 464 p., 1995.

PAYNE, R.E. Albedo of the sea-surface. **Journal of the Atmospheric Science**, v. 29, p. 959-970, 1972. doi

R CORE TEAM. **R: A Language and Environment for Statistical Computing**. R Foundation for Statistical Computing, Vienna, Austria. URL https://www.R-project.org/, 2017.

SENE, K.J.; GASH, J.H.C.; McNEIL, D.D. Evaporation from a tropical lake: comparison of theory with direct measurements. **Journal of Hydrology**, v. 127, n. 1-4, p. 193-217, 1991. doi

SHUTTLEWORTH, W.J. **Terrestrial Hydrometeorology**. Chichester: Wiley-Blackwell, 448 p., 2012.

VITALE, A.J.; GENCHI, S.A.; PICCOLO, M.C. Assessing the surface radiation balance and associated components in an intertidal wetland. **Journal of Coastal Research**, v. 35, n. 1, p. 158-164, 2019. doi

WRIGHT, J.L. New evapotranspiration crop coefficients. **Journal of Irrigation and Drainage Engineering**, v. 108, n. 1, p. 57-74, 1982. doi

WU, B.; LIU, S.; ZHU, W.; YAN, N.; XING, Q.; TAN, S. An improved approach for estimating daily net radiation over the Heihe River Basin. **Sensors**, v. 17, p. 1-18, 2017. doi